Supporting Information

Delignified Wood with Unprecedented Anti-oil Property for Highly Efficient Separation of Crude Oil/water Mixtures

Ming-Bang Wu[a], *Yong-Ming Hong*[b], *Chang Liu*[a], *Jing Yang**[a], *Xin-Ping Wang*[b], *Seema Agarwal*[c], *Andreas Greiner**[c], *and Zhi-Kang Xu**[a]

[a]MOE Key Laboratory of Macromolecular Synthesis and Functionalization, and Key Laboratory of Adsorption and Separation Materials & Technologies of Zhejiang Province, Department of Polymer Science and Engineering, Zhejiang University, Hangzhou 310027, China
[b]Department of Chemistry, Zhejiang Sci-Tech University, Hangzhou 310018, China
[c]Macromolecular Chemistry and Bavarian Polymer Institute, University of Bayreuth, Universitatsstrasse 30, Bayreuth 95440, Germany

E-mails: jing_yang@zju.edu.cn *(J. Yang);* greiner@uni-bayreuth.de *(A. Greiner);* xuzk@zju.edu.cn *(Z.-K. Xu).*

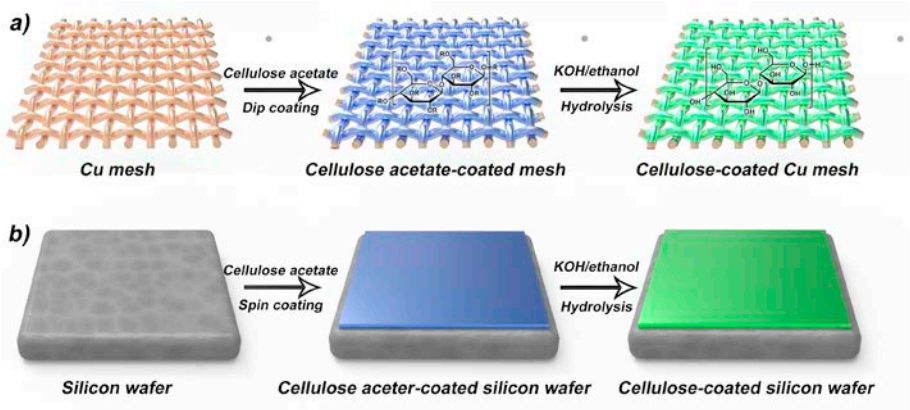

Scheme S1. Cellulose coatings can be fabricated on various substrates via a) dip or b) spin coating method (dip coating for porous substrates while spin coating for smooth and flat substrates). Here, Cu meshes and silicon wafers are chosen as the representations to show the preparation process.

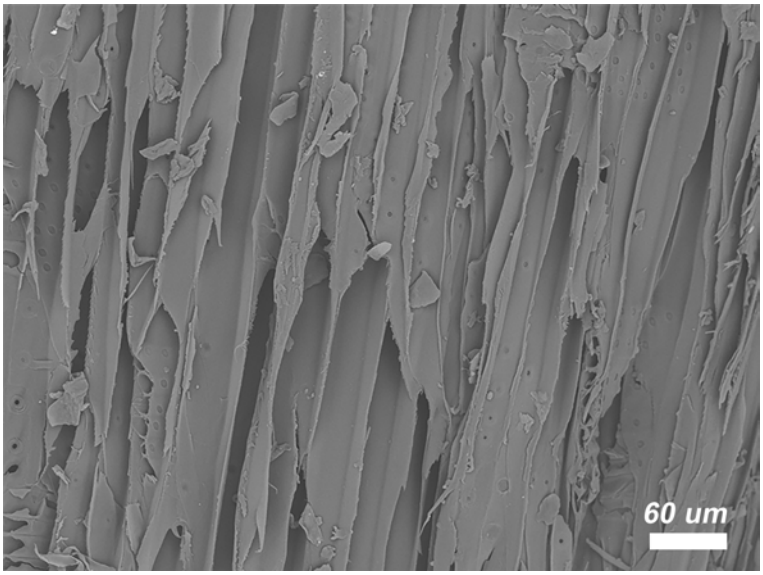

Figure S1. SEM image of the natural basswood surface that along the growth direction.

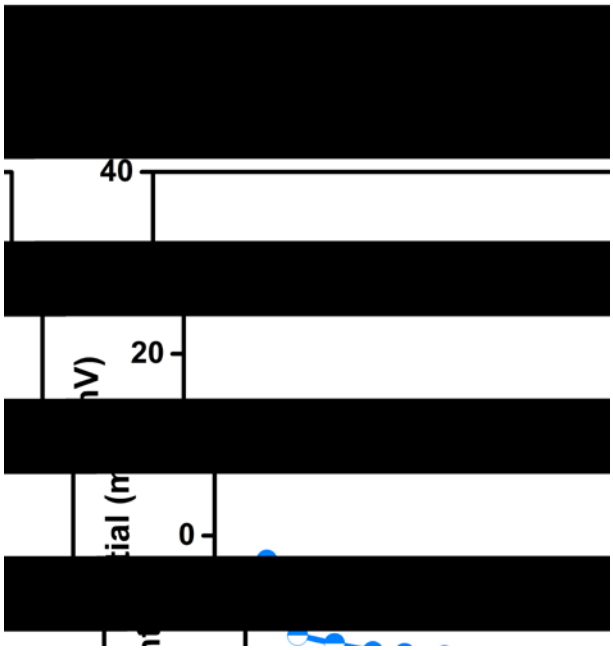

Figure S2. Zeta potential of the cellulose surfaces at different pH values. It can be seen that the Zeta potential of the cellulose surface almost keeps unchanged during the test. This indicates that there is no protonation or deprotonation for cellulose when the pH ranges from 3 to 10.

Figure S3. Microphotograph of the collected filtrate after separation by the delignified wood.

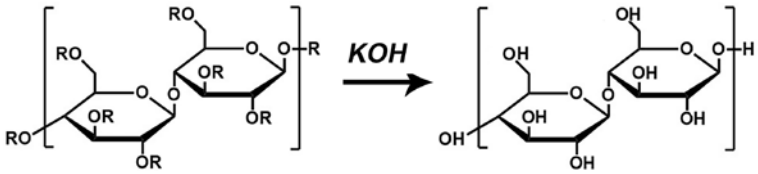

Figure S4. Chemical formula of cellulose acetate during the hydrolysis process. Cellulose is resulted from the hydrolysisof cellulose acetate.

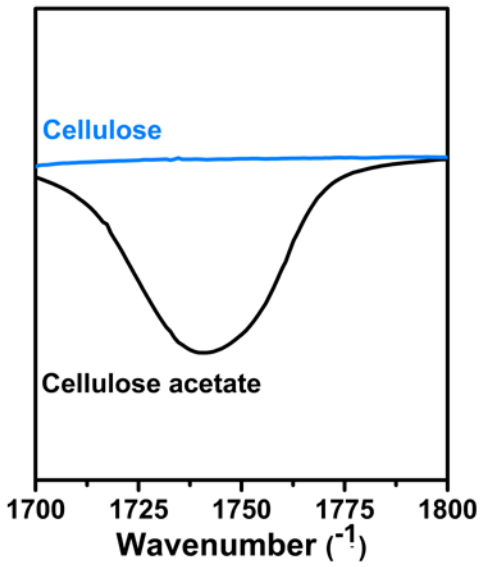

Figure S5. FT-IR spectra before and after the hydrolysis of cellulose acetate. The results show that the typical absorption peak of cellulose acetate at 1725 cm^{-1} due to the C=O stretching vibration disappears after hydrolyzing by KOH/ethanol solution, illustrating the successful formation of cellulose.

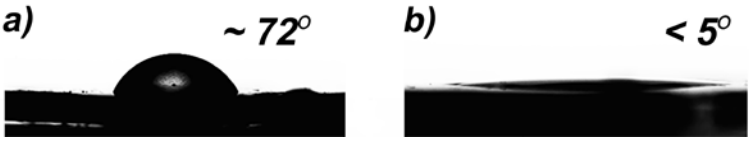

Figure S6. Static water contact angle (WCA) images of gold surface with a) cellulose acetate coating and b) cellulose coating in air, respectively. WCA is about 72° for the cellulose acetate coating on the gold surface and that is dramatically decreased to within 5°for the cellulose coating, because the hydroxyl groups in the cellulose coating have much better hydratability than acetate groups in cellulose acetate.

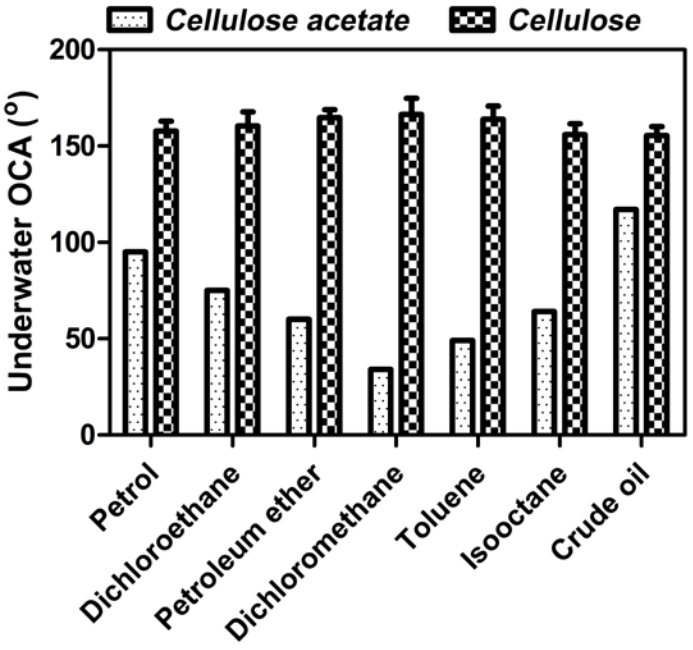

Figure S7. Underwater oil contact angle (OCA) for the cellulose acetate and cellulose coatings on the gold surfaces. The cellulose coating shows a high underwater OCA above 160° for various oils while those of the cellulose acetate coating are below 110°.

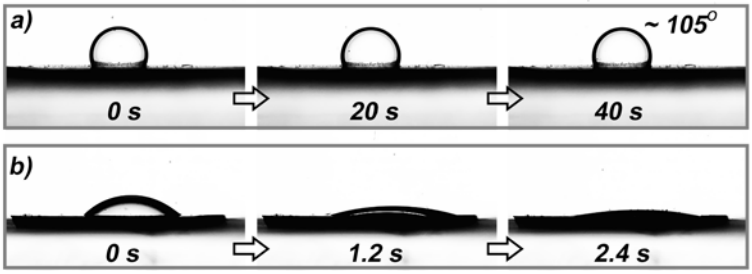

Figure S8. Dynamic optical images showing the wetting behavior with a water droplet on a) the cellulose acetate-coated gold surface, and b) the cellulose-coated gold surface in isooctane. We monitored the dynamic wetting behavior of the cellulose acetate coating and the cellulose coating in oil by a water droplet. The underoil WCA of the cellulose acetate coating is higher than 100° and the water droplet maintains unchanged during the measurement (Figure S8a). On the contrary, the water droplet on the cellulose coating surface can spread quickly within 2.4 s and the final WCA is lower than 5° as well as it is the air (Figure S8b).

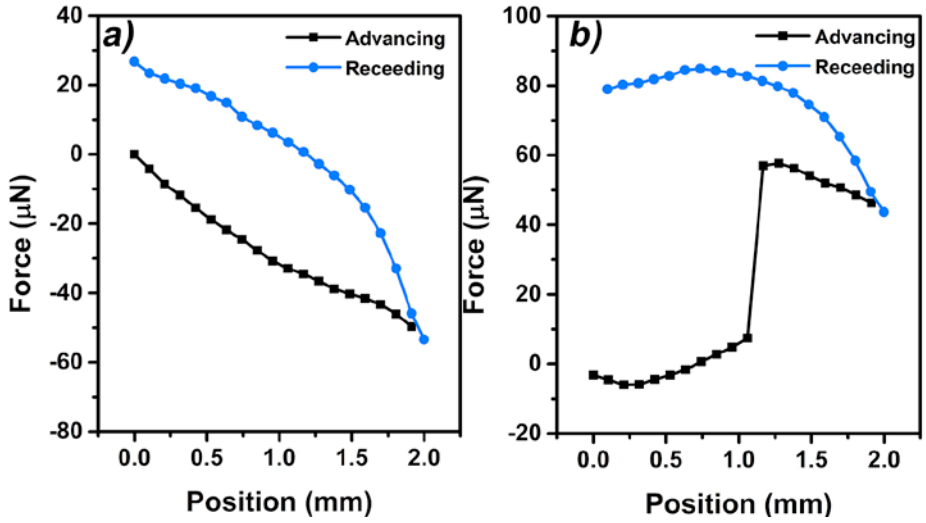

Figure S9. Force-distance curve of an underwater crude oil droplet on a) the cellulose coating and b) the cellulose acetate coating, respectively.

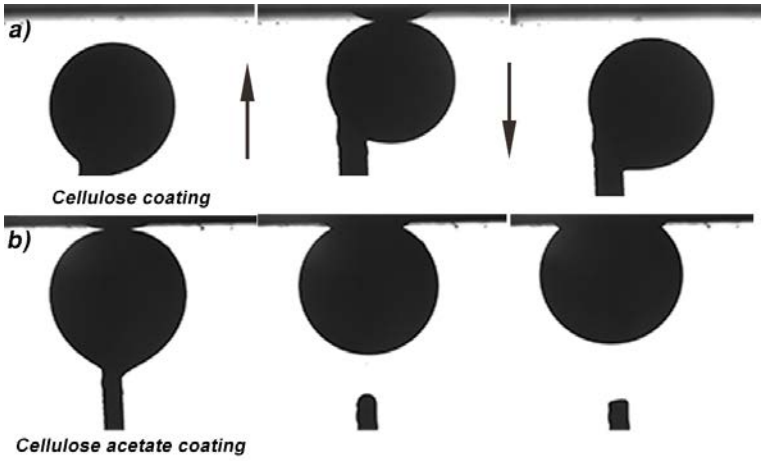

Figure S10. A series of photos taken when a crude oil droplet was approaching or leaving a) the cellulose coating and b) the cellulose acetate coating, respectively. The cellulose coating also shows ultralow underwater crude oil adhesion force around 0 μN and no oil residual is left on the cellulose coating (Figure S9a and Figure S10a). In contrast, the adhesion force is above 65 μN on the cellulose acetate coating and oil adhesion or deformation is obviously observed when the oil droplet is left from the coating surface (Figure S9b and Figure S10b).

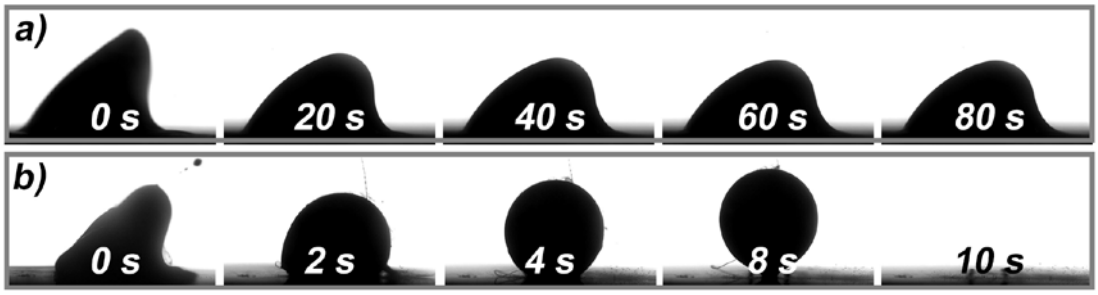

Figure S11. A series of photographs taken when a) the cellulose acetate-coated gold surface and b) the cellulose-coated gold surface, fouled by high viscosity crude oil in air, are placed into water at 60°C. The immersion time is marked in the images. Subsequently, the de-wetting behavior was compared between the cellulose coating and the cellulose acetate one by fouling their surfaces with crude oil in the air without pre-hydration and then immersing them into hot water. It can also be seen that the crude oil keeps adhering on the cellulose acetate coating without any deformation or detachment even after 80 s (Figure S11a and Movie S3). Instead, the crude oil film on the cellulose coating shrinks into a single droplet immediately within 6 s and then detaches from the coating surface at 10 s (Figure S11b and Movie S4). These results demonstrate that the cellulose coating indeed has outstanding surface hydrophilicity and oil-repellent property in both dry and pre-hydration states resulting from its outstanding water binding capability.

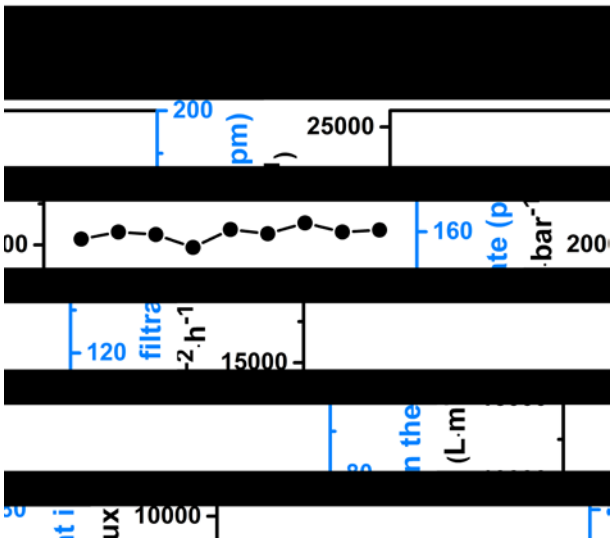

Figure S12. Water permeation flux and oil content in filtrate when separating the crude oil/water mixture with the cellulose-coated delignified wood over 9 cycles. After each cycle, the delignified wood was immersed into a clean water to remove the oil contamination. The thickness of wood used in this test is 4 mm.

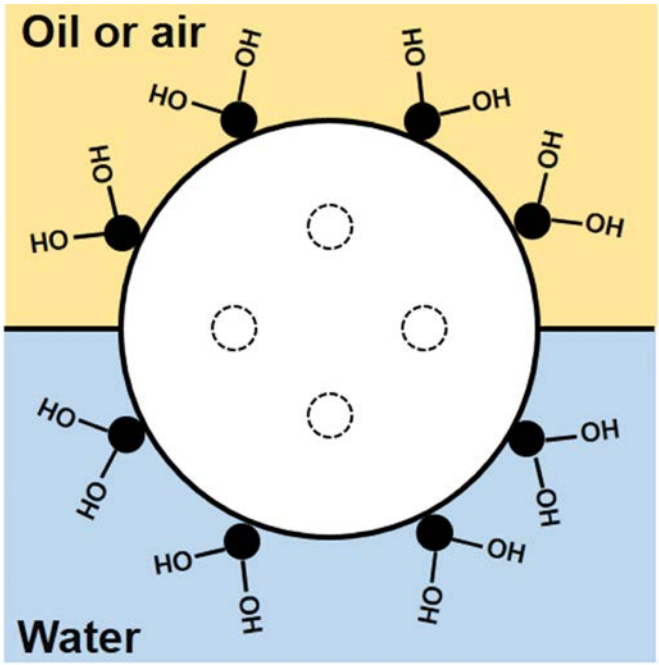

Figure S13. Projections of the cellulose chemical structure.

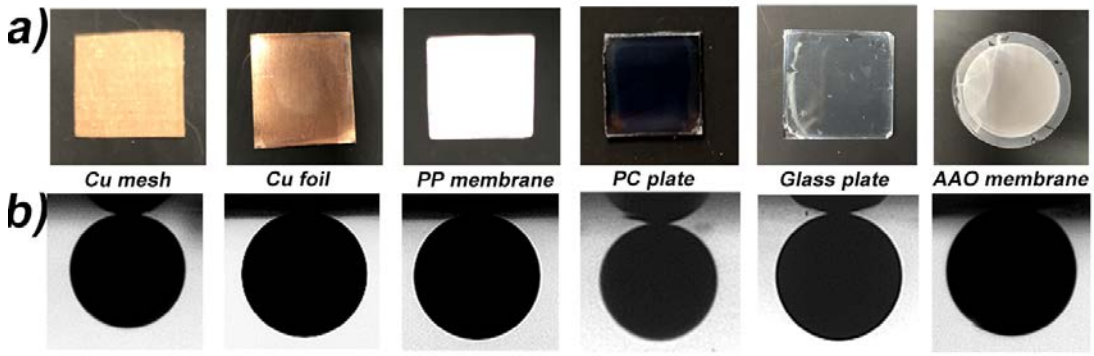

Figure S14. a) Digital photos of various cellulose-coated substrates. b) images of crude oil on corresponding substrates.

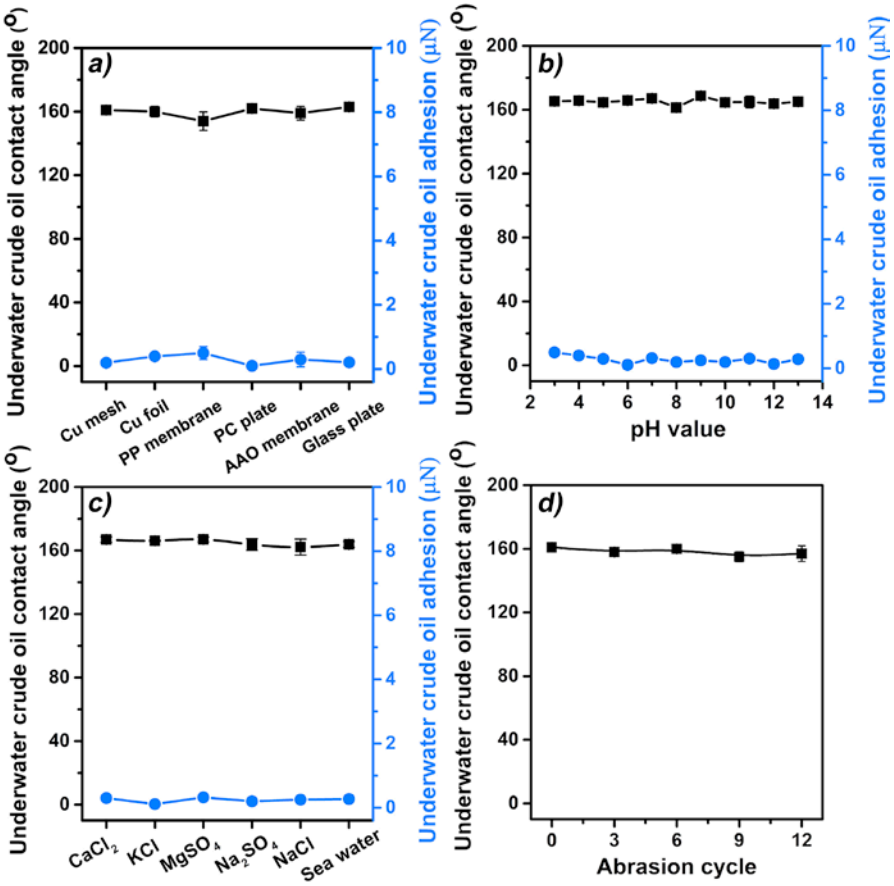

Figure S15. a) Underwater crude oil contact angle and underwater crude oil adhesive force of the cellulose coatings on different substrates. Underwater crude oil contact angle and underwater crude oil adhesive force of silicon wafer with cellulose coating measured in b) different pH values between 3 and 12, and c) salt solution containing 50 g/L of different salts. d) Underwater crude oil contact angle of cellulse-coated silicon wafer after sandpaper abrasion. The underwater crude oil contact angle was measured after three cycles abrasion tests.

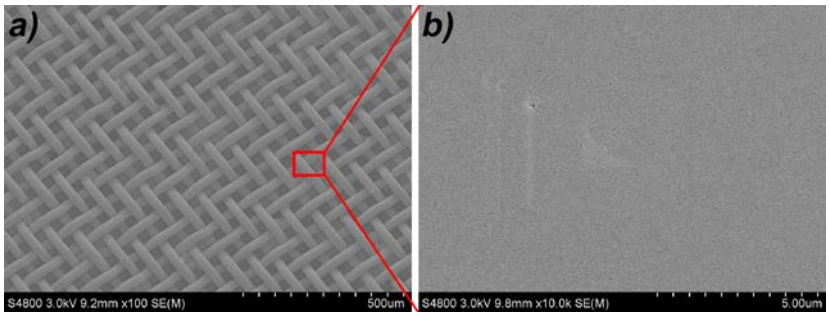

Figure S16. a) Low and b) high magnification SEM images of copper meshes with cellulose coating.

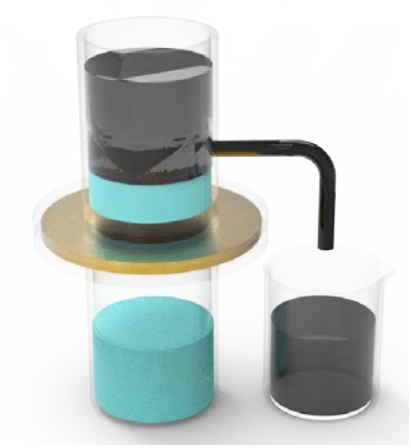

Figure S17. Schematic diagram of the home-made crude oil/water separation device while the copper meshes were used.

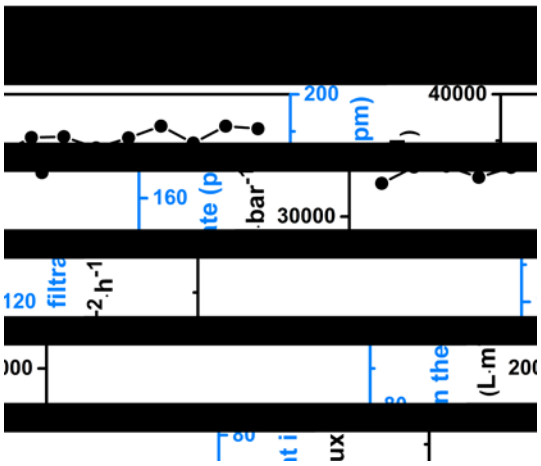

Figure S18. Water permeation flux and oil content in filtrate when separating the crude oil/water mixture with the cellulose-coated copper meshes over 9 cycles. After each cycle, the meshes were immersed into a clean water to remove the oil contamination.